Available online at www.sciencedirect.com

SciVerse ScienceDirect

Solar Energy 86 (2012) 1306–1312

SOLAR ENERGY

www.elsevier.com/locate/solener

Transmittance from visible to mid infra-red in AZO films grown by atomic layer deposition system

Tara Dhakal [a,*], Abhishek S. Nandur [a], Rachel Christian [a], Parag Vasekar [a], Seshu Desu [a,1], Charles Westgate [a], D.I. Koukis [b], D.J. Arenas [c], D.B. Tanner [b]

[a] Center for Autonomous Solar Power, Binghamton University, Binghamton, NY 13902, USA
[b] Department of Physics, University of Florida, Gainesville, FL 32611, USA
[c] Department of Physics, University of North Florida, Jacksonville, FL 32224, USA

Received 18 November 2011; accepted 26 January 2012
Available online 21 February 2012

Communicated by: Associate Editor Takhir Razykov

Abstract

We report transmittance and conductivity measurements of aluminum-doped zinc oxide films grown by atomic layer deposition. The results show that the films have 80–90% transmittance in the visible region and good transmittance in the infrared. To our knowledge, this is the first time that the transmittance of aluminum-doped zinc oxide is reported to extend beyond 2500–5000 nm. Following annealing, an optimal sheet resistance of 25 Ω/□ was obtained for a 575 nm thick film with a carrier density of 2.4×10^{20} cm^{-3} without compromising the transmittance in the visible regime.

Keywords: Aluminum-doped zinc oxide; Transparent conducting oxide; Atomic Layer Deposition; Transmittance of AZO; IR transmittance

1. Introduction

Aluminum-doped zinc oxide (AZO) is an affordable, non-toxic and robust transparent conductive oxide (TCO) (Suzuki et al., 1996). AZO has already found applications in thin film photovoltaics such as CdTe and CIGS based solar cells (Dhere et al., 2011; Vasekar et al., 2009) and is a good candidate to replace indium tin oxide (ITO), the current most popular TCO (Murdoch et al., 2009). The desire to replace ITO stems from its high production cost and the relative scarcity of indium in the earth's crust. The higher stability of AZO in reducing atmospheres may also be an advantage for future applications (Minami et al., 1989). Furthermore, AZO films are more transparent in the infrared (IR) than ITO films. IR transmission is very important because increasing the long-wavelength response is an approach to increase the efficiency of some solar devices (Berginski et al., 2007). Thus, AZO films are ideal replacements for ITO films in applications such as transparent electrodes for solar cells, flat panel displays, LCD electrodes, touch panel transparent contacts and IR windows (Park et al., 2006).

AZO thin films can be deposited by several techniques such as sol–gel (Tang and Cameron, 1994; Musat et al., 2004; Radhouane, 2005; Verma et al., 2010), chemical spray (Mondragón-Suárez et al., 2002; Islam et al., 1996), thermal evaporation (Jin et al., 1999; Ma et al., 2000), pulsed laser deposition (Singh et al., 2001; Mass et al., 2003; Agura et al., 2003; Liu and Lian, 2007), DC and RF magnetron sputtering (Berginski et al., 2007; Jeong et al., 2003; Yang et al., 2010) and reactive mid-frequency (mf, 50 kHz) magnetron sputtering using dual magnetron

* Corresponding author. Tel.: +1 6077774034; fax: +1 6077775780.
E-mail address: tdhakal@binghamton.edu (T. Dhakal).
[1] The author was affiliated to the Center for Autonomous Solar Power when the results were obtained.

0038-092X/$ - see front matter © 2012 Elsevier Ltd. All rights reserved.
doi:10.1016/j.solener.2012.01.022

cathodes (Kon et al., 2002). The desired qualities of a good TCO: transparency, conductivity, and surface texture, depend on the growth technique and the growth parameters. Atomic layer deposition (ALD) is a growth technique which has recently become very popular (Yousfi et al., 2001; Kwon, 2005; Banerjee et al., 2010; Gong et al., 2011; Saarenpää et al., 2010; Luka et al., 2011) since it provides uniform and conformal coverage and control of the thin film by atomic layer precision (George et al., 1996). This technique has the potential for solar cell applications where the deposition of solar cell layers requires good interfaces between the n-type layer and the TCO layer. The growth rate of the ZnO using our ALD system was around 12 nm/min. This growth rate is low compared to sputtering systems which can have growth rates of 15–20 nm/min for RF sputtering (Jeong et al., 2003) and around 300 nm/min for dual magnetron sputtering (Kon et al., 2002). Although the growth rate of the ALD system is relatively low, the uniformity, conformality and the compactness of the film cross-section achieved from the ALD technique are superior to those from other techniques. The low growth rate from ALD can be compensated by making roll-to-roll and batch processes viable for large scale industrial production.

Two major results have been reported here. First, the growth technique and parameters were optimized to achieve a sheet resistance as low as 25 Ω/□ for a 575 nm thick film. Our results show that annealing of the film increased the conductivity by a factor of four (100–25 Ω/□). The increase in conductivity is thought to arise from oxygen deficiencies created during the annealing process. This suggestion was corroborated by X-ray photoemission spectra (XPS) which showed that the oxygen content of the films decreased after annealing. Second, optical measurements showed that ALD-grown AZO films were very transmissive in the near-infrared. The transmittance of ALD-grown AZO films beyond 800 nm has not been reported in the literature since previous work was not focused on IR transmittance (Yousfi et al., 2001; Kwon, 2005; Banerjee et al., 2010; Gong et al., 2011; Saarenpää et al., 2010; Luka et al., 2011). For similar reasons, the transmittance of AZO films grown by any other method is not reported beyond 2500 nm; in some cases the AZO films are opaque beyond 2000 nm and in other cases the data are not shown (Berginski et al., 2007; Tang and Cameron, 1994; Musat et al., 2004; Radhouane, 2005; Verma et al., 2010; Mondragón-Suárez et al., 2002; Islam et al., 1996; Jin et al., 1999; Ma et al., 2000; Singh et al., 2001; Mass et al., 2003; Agura et al., 2003; Liu and Lian, 2007; Jeong et al., 2003; Yang et al., 2010; Kon et al., 2002; Pflug et al., 2004). In this work we show that the transmittance of the films extended at least up to 5000 nm where the float-glass substrate becomes completely opaque. Also, the transmittance in the visible region normalized to that of the substrate oscillated between 90% and 100% due to constructive and destructive interference. The interference effect in films, resembling that of a Fabry–Perot cavity, allowed the calculation of the refractive index in the visible region.

2. Experimental details

The AZO films were grown by an ALD system that utilizes sequential self-limiting surface reactions between the precursors to achieve atomic layer controlled conformal thin film growth (Elam and George, 2003). The precursors used to grow the AZO films were dimethyl zinc [$Zn(CH_3)_2$] (DMZ), trimethylaluminum [$Al(CH_3)_3$] (TMA) and water (H_2O). Di-ethyl zinc (DEZ) is also used as a precursor for zinc, but we have used DMZ since it has higher vapor pressure. The precursors were purchased from STREM chemicals. Fig. 1 shows the schematic of the growth process for the ALD system. The AZO films were grown on two different substrates; single crystal Si (100) and float-glass. The growth sequence can be understood from the following surface reactions on a hydroxylated silicon substrate. Since H_2O is adsorbed on most surfaces, a formation of Si–O–H hydroxyl group on the silicon substrate is expected.

1. $Zn(CH_3)_2 + Si–O–H = Si–O–Zn(CH_3) + CH_4$.
2. $Si–O–Zn(CH_3) + H_2O = Si–O–Zn–O–H + CH_4$.
3. $Si–O–Zn–O–H + Al(CH_3)_3 = Si–O–Zn–O–Al(CH_3)_2 + CH_4$.
4. $Si–O–Zn–O–Al(CH_3)_2 + 2H_2O = Si–O–Zn–O–Al–(O–H)_2 + 2CH_4$.

The pulse cycles of DMZ, H_2O and TMA were chosen to achieve desired compositions and thicknesses. Methane gas, the byproduct in the reaction shown above, was purged out after every cycle. Any unreacted precursor was also purged at the same time, thus self-limiting the surface reaction. Nitrogen was used as the carrier and purge gas. In the ALD method, the precursors do not react with themselves and each reaction is terminated in one layer resulting in one monolayer. Therefore, both the growth

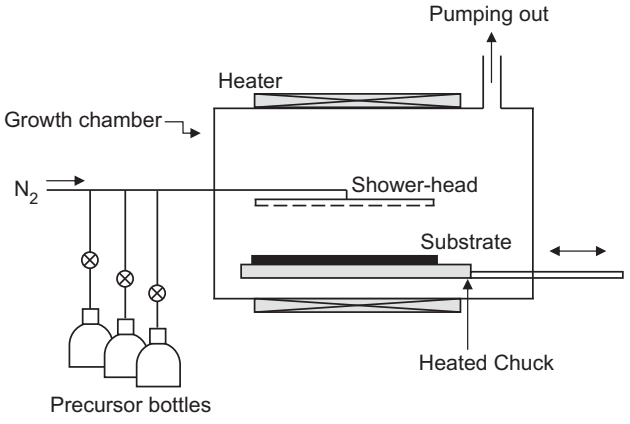

Fig. 1. Schematic of the atomic layer deposition (ALD) system.

rate and the film thickness can be precisely controlled. The duration of the DMZ and TMA cycles was kept at 125 ms, whereas the cycle duration for H_2O was kept at 175 ms to assure the formation of hydroxyl group on the surface. The purge time between each cycle of the precursors was 300 ms. The reactor was pumped to a base pressure of 1 mTorr. During the growth cycle, the pressure was 0.6 Torr. The growth rate of the AZO film was 1.95 Å/cycle with a cycle time of 1 s. As expected for ALD growth, the growth rate was linear for the films with thicknesses as high as 600 nm. The growth temperatures were varied from 150 to 325 °C. The films grown at 325 °C had the best crystalline quality and the highest conductivity.

The ratio of DMZ and TMA (amount of doping) pulse cycles were varied to improve the conductivity of the AZO film. The pulsing of 1 TMA cycle after every 20 DMZ pulse cycles produced the AZO films with the highest conductivities. The energy dispersive X-ray analysis (EDX) confirmed that this ratio corresponded to 3 atomic percent (at.%). The surface morphology of the as-grown thin films was imaged using a Scanning Electron Microscope (SEM). The films were relatively smooth with uniform distribution of grains of 60–100 nm length and 10–20 nm width (Fig. 2). The XRD spectra of the film showed all the characteristics of the ZnO hexagonal lattice with space group $P6_3mc$ (186). No trace of impurity peaks were observed even in the logarithmic scale. The film texture was predominantly (100) oriented (Fig. 3). The film resistances were measured by the standard 4-probe technique and the carrier concentrations were studied by Hall Effect measurements using a Van der Paw geometry.

3. Results

3.1. Optimization of sheet resistance by annealing

For conductivity measurements, AZO films were grown on Si (100) with a 20 nm thick buffer layer of Al_2O_3. The thick buffer layer allowed an accurate measurement of the conductivity of the AZO film. The 575 nm thick AZO film grown at 325 °C had a sheet resistance of 100 Ω/□ and a carrier concentration of $1.86 \times 10^{20}/cm^3$. The conductivity of the film was improved by rapid thermal annealing in argon (95%)–hydrogen (5%) ambient at temperatures ranging from 350 °C to 600 °C for 5 min; and the optimal annealing temperature was 400 °C. Since the films annealed at 400 °C showed the lowest sheet resistance, the films were further annealed at this temperature at varying times. The lowest sheet resistance of 25 Ω/□ was observed for 30 min annealed film (Table 1). The optimal sheet resistance of 25 Ω/□ for the 575 nm thick film corresponded to a resistivity of 1.4×10^{-3} Ω.cm. This value of the conductivity is comparable to the highest conductivity films grown by ALD (Kwon, 2005; Banerjee et al., 2010; Saarenpää et al., 2010; Luka et al., 2011) and other methods (Musat et al., 2004; Singh et al., 2001; Mass et al., 2003; Liu and Lian, 2007).

The improvement in conductivity in the AZO film after annealing may be attributed to oxygen deficiency created from annealing in a reducing environment. The annealing process also improved the smoothness of the film. The decrease in roughness may have also contributed to the slight decrease in the sheet resistance. Atomic force

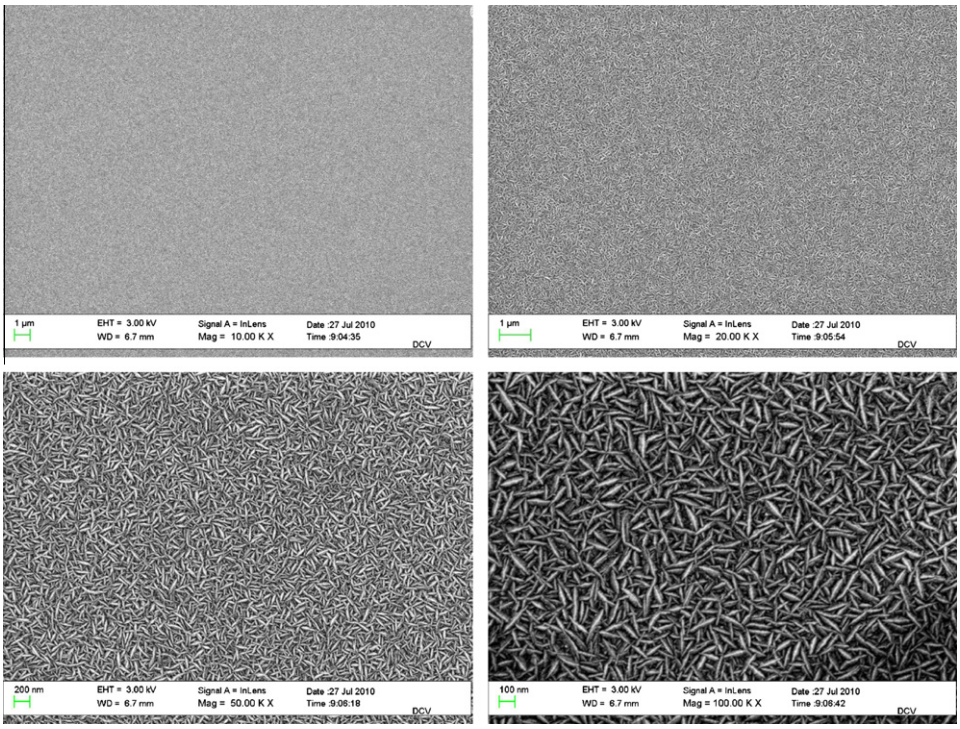

Fig. 2. SEM images at varying magnifications of the AZO films grown on Si(100).

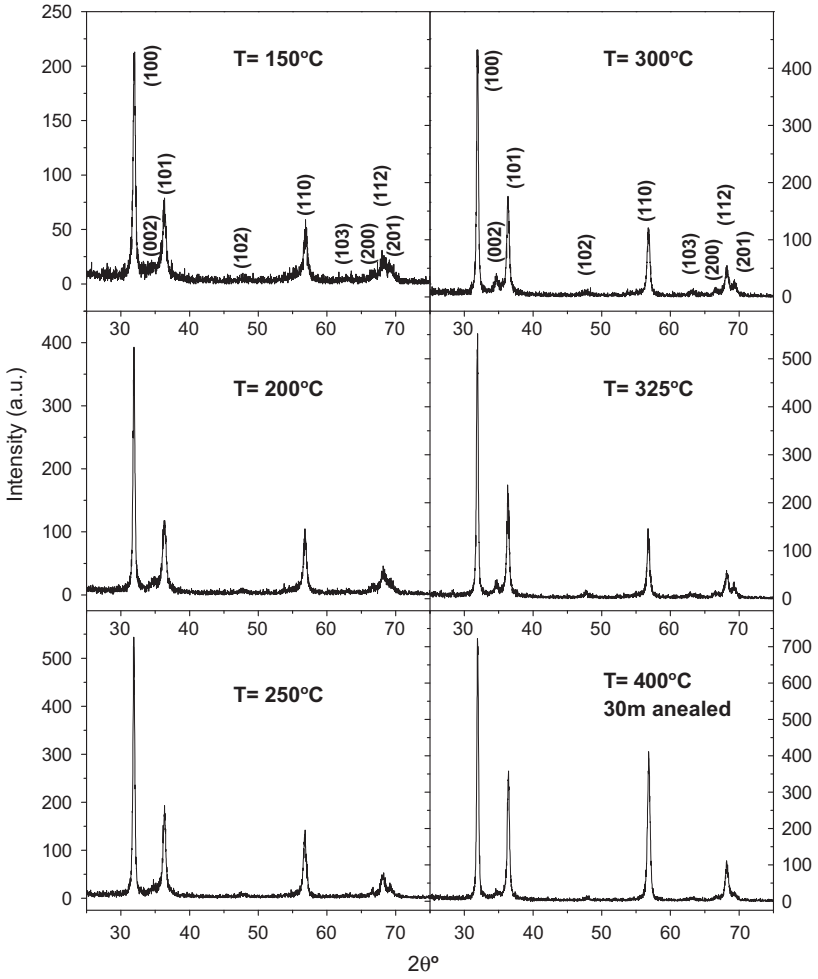

Fig. 3. XRD peaks of AZO thin films grown at 150–325 °C and annealed 30 m in argon.

Table 1
Electrical characteristics of the 575 nm thick AZO film annealed in argon–hydrogen atmosphere at 400 °C and at different times using Hall-effect measurement.

Annealing time (min)	Sheet resistance R_S (Ω/□)	Resistivity ρ (Ω.cm)	Carrier density (n/cm^3)	Mobility μ (cm^2 V^{-1} s^{-1})	Carrier type
0	97.77	5.623E−03	1.86E+20	6.51	n-type
5	32.67	1.879E−03	2.56E+20	13.18	n-type
30	25.95	1.492E−03	2.39E+20	17.76	n-type
60	30.87	1.775E−03	2.62E+20	13.53	n-type

microscopy (AFM) imaging of the 30 min-annealed films showed that the roughness decreased from 7.31 nm to 6.72 nm after annealing.

3.2. X-ray photoelectron spectroscopy measurements

The films were studied using X-ray photoelectron spectroscopy (XPS) to gain insight into the possible oxygen deficiencies caused by annealing. XPS was performed by irradiating the sample with monochromatic Al Kα X-rays of energy 1486 eV. Fig. 4 shows the survey scan of an 30 min-annealed film. The observed XPS peaks are related to Zn2p3/2, oxygen O1s, Al2p and the common environmental contaminant carbon C1s. Other peaks were also observed. The carbon C1s line was designated to 284.8 eV (standard position) and the spectrum was shifted accordingly. The Zn 2p3/2 binding energy of 1021.8 eV and the oxygen O1S binding energy of 530.8 eV are associated with the zinc oxide (ZnO) structure (Battistoni et al., 1981; Langer and Vesely, 1970). The Al 2p binding energy of 73.32 eV makes it difficult to determine its exact oxidation state, but it is not associated with Al_2O_3 (Arata and Hino, 1990). Elemental analysis was performed on films before annealing and after the 30 min annealing. The film surface was argon-etched until the carbon C1s peak due to the carbon contaminant disappeared. The elemental composition is depicted in the table in the inset of Fig. 4. The XPS results show that the oxygen content is reduced for the annealed film. The conductivities of the AZO films depend on the oxygen vacancy concentration in addition to aluminum doping. Oxygen vacancies give rise to dangling Zn bonds and increasing conductivity as shown in Table 1. It is also possible that the reduced roughness in the annealed film further improved the conductivity. However,

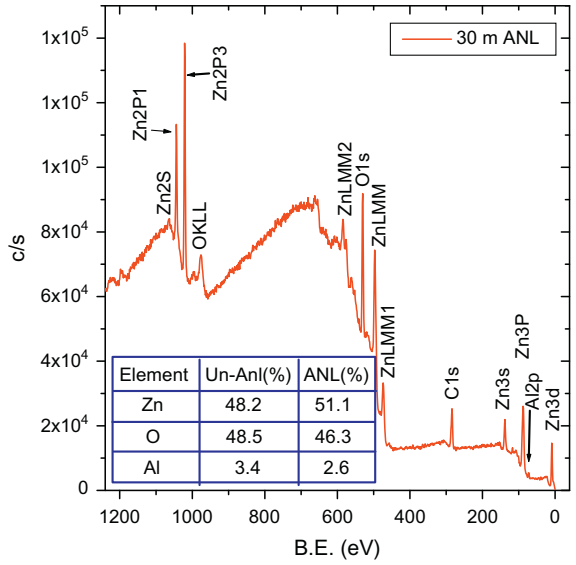

Fig. 4. XPS spectrum of 30 m-annealed AZO film. The inset shows the elemental composition of Zn, O and Al obtained from the Zn2P3, O1s and Al2P spectral lines respectively for annealed and un-annealed samples.

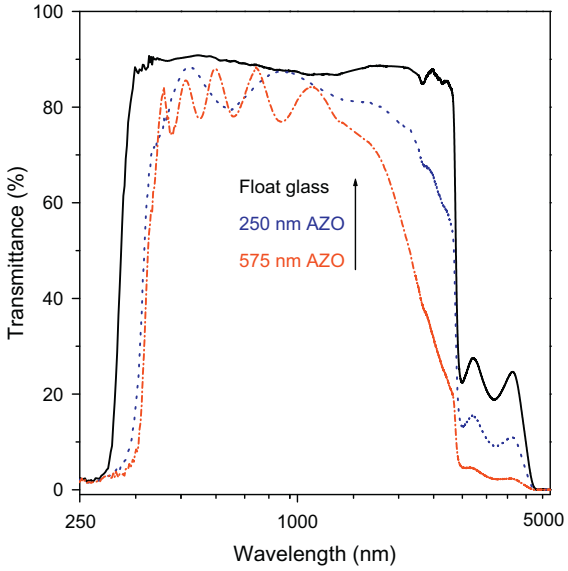

Fig. 5. Transmission spectra of the 250 nm and 575 nm AZO films grown on float glass. For comparison, float glass transmission is also shown.

as the annealing time increased, the resistance of the film started to increase (Table 1), which could be due to the increase in residual oxygen partial pressure arising from the oxygen impurity present in the argon gas and unavoidable leaks in the system.

3.3. Transmittance measurements

The transmittance of the AZO films grown on float-glass was measured in the 250–5000 nm wavelength range. Two different thicknesses (250 and 575 nm) were measured. The transmittance was measured in the mid-infrared to ultraviolet range by using a spectrophotometer (0.25–0.85 μm), a Perkin Elmer 16U grating spectrometer (0.4–3 μm), and a Bruker 113 v Fourier Spectrometer (2–20 μm). The transmittance measured with the different spectrometers overlapped well and yielded an uncertainty of ±1%. A new observation is that the AZO films were transmissive in the IR up to 5 μm. The transmittance in the infrared of the film/substrate would extend farther if it were not limited by the substrate cut-off. The transmittance of AZO above 2 μm is another advantage of AZO over ITO - since the latter is opaque beyond 2 μm. In the visible part of the spectrum, the transmittance of both the 250 nm and 575 nm thick films were in the range of 80–90% (Fig. 5), which corresponded to a normalized transmittance of 90–100%.

The transmittance also showed oscillations in the visible region. A simple analysis of this interference effect can give further insight into the optical properties of these films in this part of the spectrum. These oscillations correspond to constructive and destructive interference between multiple bounce beams and these can be used to calculate the refractive index (Hecht, 2001). Since the spacing between the transmittance maxima (Δf) is related to the film thickness d by

$\Delta f = 1/(2n*d)$, the refractive index n can be estimated. The maxima spacing Δf of 9000 cm^{-1} and 4000 cm^{-1} for the 250 and 575 nm films respectively yielded a refractive index of 2 for both films in the 0.4–1.2 μm region of the spectrum (Fig. 6). This value is in agreement with the value for a ZnO based system (Heideman et al., 1995).

The oscillations also yielded information about the absorption and the imaginary part of the refractive index. At a frequency corresponding to a maximum, the outgoing and back-reflected waves all add in phase. If the film has no absorption, then all the light should be transmitted at a frequency where there is constructive interference. The fact that the normalized transmittance equals one at a maximum shows that the absorption from the film itself is negligible in this spectral region.

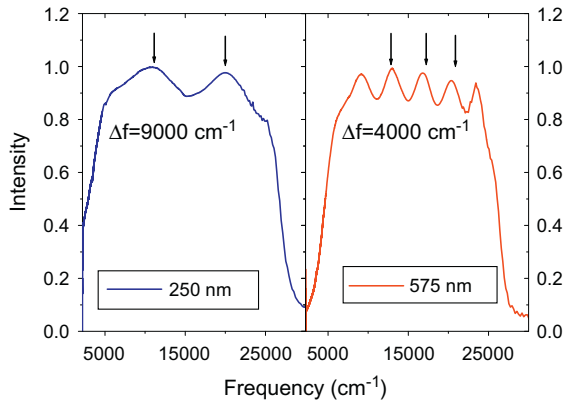

Fig. 6. Transmission spectra divided over that of float glass as a function of frequency. The spacing between the transmittance maxima (due to constructive interference) are used to calculate the refractive indices for both films at that range of the spectrum.

4. Conclusions

Highly conductive and transparent AZO films were grown using atomic layer deposition. The conductivity of the film was further improved by post deposition annealing. An optimum sheet resistance of 25 Ω was obtained after annealing of the films at 400 °C in argon ambient. XPS measurements showed that oxygen deficiencies caused by annealing may be responsible for the increase in conductivity. In the visible spectrum, the normalized transmittance was between 90% and 100%, and the films were shown to be transmissive up to 5000 nm. Further measurements on the optical transmittance of the AZO films on substrates with a better IR window are on the way.

Acknowledgments

This work was supported in part by Defense Advanced Research Projects Agency (DARPA) Award Number HR0011101002. The authors would like to thank Daniel Vanhart for SEM imaging and David Spencer for XPS measurements performed at the Analytical and Diagnostic Lab (ADL) at the Binghamton University. Research at the University of Florida was supported by the US. Department of Energy through contract No. DE-FG0202ER45984.

References

Agura, H., Suzuki, A., Matsushita, T., Aoki, T., Okuda, M., 2003. Low resistivity transparent conducting Al-doped ZnO films prepared by pulsed laser deposition. Thin Solid Films 445, 263–267.

Arata, K., Hino, M., 1990. Solid catalyst treated with anion: XVIII. Benzoylation of toluene with benzoyl chloride and benzoic anhydride catalysed by solid superacid of sulfate-supported alumina. Appl. Catal. 59, 197–204.

Banerjee, P., Lee, W., Bae, K., Lee, S.B., Rubloff, G.W., 2010. Structural, electrical, and optical properties of atomic layer deposition Al-doped ZnO films. J. Appl. Phys. 108, 043504.

Battistoni, C., Dormann, J.L., Fiorani, D., Paparazzo, E., Viticoli, S., 1981. An XPS and Mössbauer study of the electronic properties of $ZnCrxGa_{2-x}O_4$ spinel solid solutions. Solid State Commun. 39, 581–585.

Berginski, M., Hupkes, J., Schulte, M., Schope, G., Stiebig, H., Rech, B., Wuttig, M., 2007. The effect of front ZnO:Al surface texture and optical transparency on efficient light trapping in silicon thin-film solar cells. J. Appl. Phys. 101, 074903.

Dhere, R.G., Bonnet-Eymard, M., Charlet, E., Peter, E., Duenow, J.N., Li, J.V., Kuciauskas, D., Gessert, T.A., 2011. CdTe solar cell with industrial Al:ZnO on soda-lime glass. Thin Solid Films 519, 7142–7145.

Elam, J.W., George, S.M., 2003. Growth of ZnO/Al_2O_3 alloy films using atomic layer deposition techniques. Chem. Mater. 15, 1020–1028.

George, S.M., Ott, A.W., Klaus, J.W., 1996. Surface chemistry for atomic layer growth. J. Phys. Chem. 100, 13121–13131.

Gong, S.C., Jang, J.G., Chang, H.J., Park, J., 2011. The characteristics of organic light emitting diodes with Al doped zinc oxide grown by atomic layer deposition as a transparent conductive anode. Synth. Met. 161, 823–827.

Hecht, E., 2001. Optics, fourth ed. Addison Wesley.

Heideman, R.G., Lambeck, P.V., Gardeniers, J.G.E., 1995. High quality ZnO layers with adjustable refractive indices for integrated optics applications. Opt. Mater 4, 741–755.

Islam, M.N., Ghosh, T.B., Chopra, K.L., Acharya, H.N., 1996. XPS and X-ray diffraction studies of aluminum-doped zinc oxide transparent conducting films. Thin Solid Films 280, 20–25.

Jeong, S.H., Lee, J.W., Lee, S.B., Boo, J.H., 2003. Deposition of aluminum-doped zinc oxide films by RF magnetron sputtering and study of their structural, electrical and optical properties. Thin Solid Films 435, 78–82.

Jin, M., Feng, J., De-heng, Z., Hong-lei, M., Shu-ying, L., 1999. Optical and electronic properties of transparent conducting ZnO and ZnO:Al films prepared by evaporating method. Thin Solid Films 357, 98–101.

Kon, M., Song, P.K., Shigesato, Y., Frach, P., Mizukami, A., Suzuki, K., 2002. Al-doped ZnO films deposited by reactive magnetron sputtering in mid-frequency mode with dual cathodes. Jpn. J. Appl. Phys. 41, 814–819.

Kwon, S.J., 2005. Effect of precursor-pulse on properties of Al-doped ZnO films grown by atomic layer deposition. Jpn. J. Appl. Phys. 44, 1062–1066.

Langer, D.W., Vesely, C.J., 1970. Electronic core levels of Zinc chalcogenides. Phys. Rev. B 2, 4885–4892.

Liu, Y., Lian, J., 2007. Optical and electrical properties of aluminum-doped ZnO thin films grown by pulsed laser deposition. Appl. Surf. Sci. 253, 3727–3730.

Luka, G., Wachnicki, L., Witkowski, B.S., Krajewski, T.A., Jakiela, R., Guziewicz, E., Godlewski, M., 2011. The uniformity of Al distribution in aluminum-doped zinc oxide films grown by atomic layer deposition. Mater. Sci. Eng. B 176, 237–241.

Ma, J., Ji, F., Ma, H., Li, S., 2000. Preparation and properties of transparent conducting zinc oxide and aluminium-doped zinc oxide films prepared by evaporating method. Sol. Energy Mater. Sol. Cells 60, 341–348.

Mass, J., Bhattacharya, P., Katiyar, R.S., 2003. Effect of high substrate temperature on Al-doped ZnO thin films grown by pulsed laser deposition. Mater. Sci. Eng.: B 103, 9–15.

Minami, T., Sato, H., Nanto, H., Takata, S., 1989. Heat treatment in hydrogen gas and plasma for transparent conducting oxide films such as ZnO, SnO_2 and indium tin oxide. Thin Solid Films 176, 277–282.

Mondragón-Suárez, H., Maldonado, A., Olvera, M.d.l.L., Reyes, A., Castanedo-Pérez, R., Torres-Delgado, G., Asomoza, R., 2002. ZnO:Al thin films obtained by chemical spray: effect of the Al concentration. Appl. Surf. Sci. 193, 52–59.

Murdoch, G.B., Hinds, S., Sargent, E.H., Tsang, S.W., Mordoukhovski, L., Lu, Z.H., 2009. Aluminum doped zinc oxide for organic photovoltaics. Appl. Phys. Lett. 94, 213301.

Musat, V., Teixeira, B., Fortunato, E., Monteiro, R.C.C., Vilarinho, P., 2004. Al-doped ZnO thin films by sol–gel method. Surf Coat technol 180–181, 659–662.

Park, S., Ikegami, T., Ebihara, K., 2006. Growth of transparent conductive Al-doped ZnO thin films and device applications. Jpn. J. Appl. Phys. 45, 8453–8456.

Pflug, A., Sittinger, V., Ruske, F., Szyszka, B., Dittmar, G., 2004. Optical characterization of aluminum-doped zinc oxide films by advanced dispersion theories. Thin Solid Films 455–456, 201–206.

Radhouane, B.H.T., 2005. Structural and electrical properties of aluminum-doped zinc oxide films prepared by sol–gel process. J. Eur. Ceram. Soc 25, 3301–3306.

Saarenpää, H., Niemi, T., Tukiainen, A., Lemmetyinen, H., Tkachenko, N., 2010. Aluminum doped zinc oxide films grown by atomic layer deposition for organic photovoltaic devices. Sol. Energy Mater. Sol. Cells 94, 1379–1383.

Singh, A.V., Mehra, R.M., Buthrath, N., Wakahara, A., Yoshida, A., 2001. Highly conductive and transparent aluminum-doped zinc oxide thin films prepared by pulsed laser deposition in oxygen ambient. J. Appl. Phys. 90, 5661–5665.

Suzuki, A., Matsushita, T., Wada, N., Sakamoto, Y., Okuda, M., 1996. Transparent conducting Al-doped ZnO thin films prepared by pulsed laser deposition. Jpn. J. Appl. Phys. 35, L56–L59.

Tang, W., Cameron, D.C., 1994. Aluminum-doped zinc oxide transparent conductors deposited by the sol-gel process. Thin Solid Films 238, 83–87.

Vasekar, P.S., Dhere, N.G., Moutinho, H., 2009. Development of CIGS2 solar cells with lower absorber thickness. Sol. Energy 83, 1566–1570.

Verma, A., Khan, F., Kumar, D., Kar, M., Chakravarty, B.C., Singh, S.N., Husain, M., 2010. Sol–gel derived aluminum doped zinc oxide for application as anti-reflection coating in terrestrial silicon solar cells. Thin Solid Films 518, 2649–2653.

Yang, W., Wu, Z., Liu, Z., Pang, A., Tu, Y., Feng, Z.C., 2010. Room temperature deposition of Al-doped ZnO films on quartz substrates by radio-frequency magnetron sputtering and effects of thermal annealing. Thin Solid Films 519, 31–36.

Yousfi, E.B., Weinberger, B., Donsanti, F., Cowache, P., Lincot, D., 2001. Atomic layer deposition of zinc oxide and indium sulfide layers for Cu(In, Ga)Se2 thin-film solar cells. Thin Solid Films 387, 29–32.